Proceedings of the 4th International Conference on Materials Chemistry and Environmental Engineering
DOI: 10.54254/2755-2721/61/20240921

Melanin nanoparticles scavenging reactive oxygen and nitrogen radicals for rheumatoid arthritis treatment

Zekun Lang

Beijing 21st Century International School, Beijing, China

langzekun01@163.com

Abstract. Rheumatoid arthritis (RA) is a complex and chronic disease that often causes long-term pain and joint swelling in patients, and even causes joint deformity and dysfunction. The pathogenesis of this disease involves abnormal activity of the immune system, causing immune cells to attack the body's joint tissues, which triggers an inflammatory response. During these inflammatory processes, the accumulation of reactive oxygen and nitrogen species (RONS) is considered to be one of the key factors that aggravate inflammation and damage joint tissues. To address this problem, we designed a method that takes advantage of the targeting properties of melanin nanoparticles. These nanoparticles have excellent biocompatibility, can remain stable in the body, and can be accurately targeted to the site of inflammation. In addition, these nanoparticles also have strong free radical scavenging ability, which can effectively neutralize excessive RONS, reduce the inflammatory response and weaken joint tissue damage. The promise of this treatment strategy is encouraging and offers new hope for patients with RA. By reducing inflammation, protecting joint tissue, and possibly even reversing the disease process to some extent, this melanin nanoparticle holds great promise.

Keywords: Rheumatoid arthritis, Reactive oxygen and nitrogen species scavenge, Targeted therapy, Melanin nanoparticles

1. Introduction

Rheumatoid arthritis (RA) is a chronic, autoimmune systemic disease characterized by inflammatory synovitis, which can lead to joint deformity and loss of function [1, 2]. In 2017 alone, RA resulted in over 47,000 deaths [3]. The typical pathology of RA includes synovitis, synovial hyperplasia, pannus, cartilage and bone destruction. However, due to certain limitations in existing treatments, such as providing only pain relief without curing the disease thoroughly [4], RA is in urgent need of new treatment methods. Traditional drugs, such as DMARD and NSAID, may even cause further damage [5].

Persistent chronic inflammation is characteristic of RA, mainly due to the interaction of factors in the RA microenvironment (RAM) during RA-related biological processes [6, 7]. Therefore, regulating RAM is important for developing targeted treatments of RA. It is often difficult for conventional drugs to effectively target many of the morbific factors because they have challenges accumulating at the joint and can cause significant side effects, leading to inefficient treatment of rheumatoid arthritis. Nanomaterials can efficiently trap or capture a variety of pathogenic agents and free radicals in RAM due to their distinctive configurational synthetic and outside particularities [8]. In addition,

DOI: 10.54254/2755-2721/61/20240921

nanomaterials can leverage enhanced permeability and retention effects for passive targeting, and utilize specific positive targeting to enhance therapeutic effectiveness, which makes them capable for the RA treatment, making them suitable for RA treatment. One of the most influential factors is the vicious cycle caused by reactive oxygen species (RONS) and endogenous inflammatory factors [9, 10]. More specifically, antibodies produced by B cells, including rheumatoid factors (RF), activate macrophages and other inflammatory cells. Activated inflammatory cells will secrete a large number of inflammatory cytokines such as TNF-α and interleukin-6 (IL-6), resulting in the overproduction of RONS in RA joints. Subsequently, RONS directly or indirectly promote the release of inflammatory mediators, leading to a vicious cycle between oxidative stress and inflammation [11]. For example, RONS can induce synovial fibroblasts to enter a proliferative state, causing synovial tissue hyperplasia. RONS are also responsible for chondrocyte apoptosis and osteoclast production, resulting in bone damage. Therefore, controlling RONS in RAM is a new method and means to effectively manage RA [12, 13].

Dopamine is naturally present in organisms and exhibits good biocompatibility and bioregeneration, so it has potential for biomedical applications [14]. Moreover, melanin, a heterogeneous biopolymer found in most organisms, including humans, exhibits photoacoustic signals, strong chelation of metal ions, and near-infrared absorption properties [15, 16]. On top of that, melanin contains a large number of functional groups, such as catecholins, amines, and imines, that scavenge free radical. Therefore, Nakajima and Kitamura stated that melanin can scavenge free radicals and can be used in research to explore its potential for treating RONS-related diseases *in vivo* [10]. In addition, the targeted release of dopamine molecules can control pathological RAM and improve treatment outcomes. Therefore, the utilization of dopamine nanoparticles with their free radical scavenging ability has emerged as a novel method to treat RA [17].

In this study, the addition of polyethylene glycol (PEG) and folic acid (FA) groups to melanin nanoparticles (MeNPs) improved the targeting ability and RONS scavenging ability of MeNPs-PEG-FA nanoparticles. Our new approach uses the binding between FA and macrophages' FA receptors to achieve the delivery to the inflammatory site. MeNPs-PEG-FA have several outstanding properties. First, MeNPs-PEG-FA are capable of clearing RONS, thereby reducing oxidative stress and inflammation associated with RA symptom. Moreover, the effect of scavenging free radicals of our systhesized dopamine molecule is markedly effective, and it can also inhibit the regulatory amounts of inflammatory factors such as TNF-α and IL-6. Therefore, MeNPs-PEG-FA nanoparticles function as RONS scavengers and inhibitory agents, showing promise as candidates for the treatment of RA. In the near future, MeNPs-PEG-FA is expected to become a new drug for RA treatment.

2. Materials and Experiment

2.1. Materials

All chemicals were of analytical grade and used without further purification. Dopamine hydrochloride, Tris(hydroxymethyl)aminomethane, and ethanol were purchased from Sinopharm Chemical Reagent Co., Ltd. (Shanghai, China). Poly (ethylene glycol) modified with FA and succinimidyl ester at each end (FA-PEG5000-NHS, Mn ≈ 5000 Da) and Poly (ethylene glycol) methyl ether modified with succinimidyl ester (mPEG5000-NHS, Mn ≈ 5000 Da) were obtained from Ponsure Biotechnology. Deionized (DI) water used in all experiments had a resistivity of 18.2 MΩ cm, and was obtained from a Milli-Q system (Millipore).

2.2. Characterization

For TEM sample grids were examined using a transmission electron microscope (TEM, Tecnai G2 F20). UV-vis-NIR absorption spectra were obtained with a shimadzu UV-1280 spectrophotometer. The zeta potentials and hydrodynamic diameters of samples were measured using a dynamic light scattering (Malvern Instruments). Fourier transform infrared (FT-IR) spectroscopy was recorded on a FTIR spectrometer (Thermo Fisher).

DOI: 10.54254/2755-2721/61/20240921

2.3. Synthesis of melanin nanoparticles (MeNPs)

As shown in the **Figure 1**, the initial step involved mixing 3 mL of ammonia solution (NH_4OH, 28-30%) with 40 mL of ethanol and 90 mL of deionized water at an optimal temperature of 30 °C, setting the stage for the forthcoming chemical reactions. The tenderly stirring for 30 minutes ensured a homogeneous distribution of the components. In parallel, the introduction of 0.5 g of dopamine hydrochloride into 10 mL of deionized water created a potent elixir that held the key to the metamorphosis. Instantaneously, the solution's color underwent a metamorphosis, transitioning from its original appearance to a light-yellow color. The significance of time in this process cannot be understated, allowing the reaction to proceed for a full 24 hours [18]. The adequate period of reaction could facilitate the growth and stabilization of the MeNPs, ensuring they reached their full size and properties. Upon completion of this period, the MeNPs were obtained through a process of centrifugation and washing with water. This process was repeated three times to ensure the purity of the MeNPs and eliminate any remaining residual components.

2.4. Synthesis of folic acid Melanin nanoparticles (MeNPs-PEG-FA/ MeNPs-mPEG)

The study commenced by dispersing precisely two portions of 50 mg MeNPs into two well-defined tris buffer solution (16 mM, pH 8.5). This step was critical to create an appropriate condition for the ensuing reactions since the productive rate could be enhanced under the basic solution condition. Subsequently, 125 mg of FA-PEG5k-NH_2 was added to one container while 125 mg of mPEG5K-NH_2 was added to another, triggering a chemical reaction that would unveil the distinctive properties of the two groups. For the next step, the mixture was constantly stirred for a duration of 12 hours, maintaining a stable room temperature environment. This prolonged incubation allowed for complete and thorough interactions between the MeNPs and the FA-PEG5k-NH_2 or mPEG5K-NH_2 components, which would govern the subsequent targeting characteristics of the nanoparticles. Following the reaction period, the synthesized MeNPs-mPEG or MeNPs-PEG-FA underwent a process of purification to eliminate any remnants of mPEG5K-NH_2 or FA-PEG5k-NH_2 from the reaction. The next step involved three cycles of centrifugation and thorough washing with deionized water to remove of any residual impurities. The MeNPs-mPEG or MeNPs-PEG-FA were redispersed in deionized water for further investigation [19].

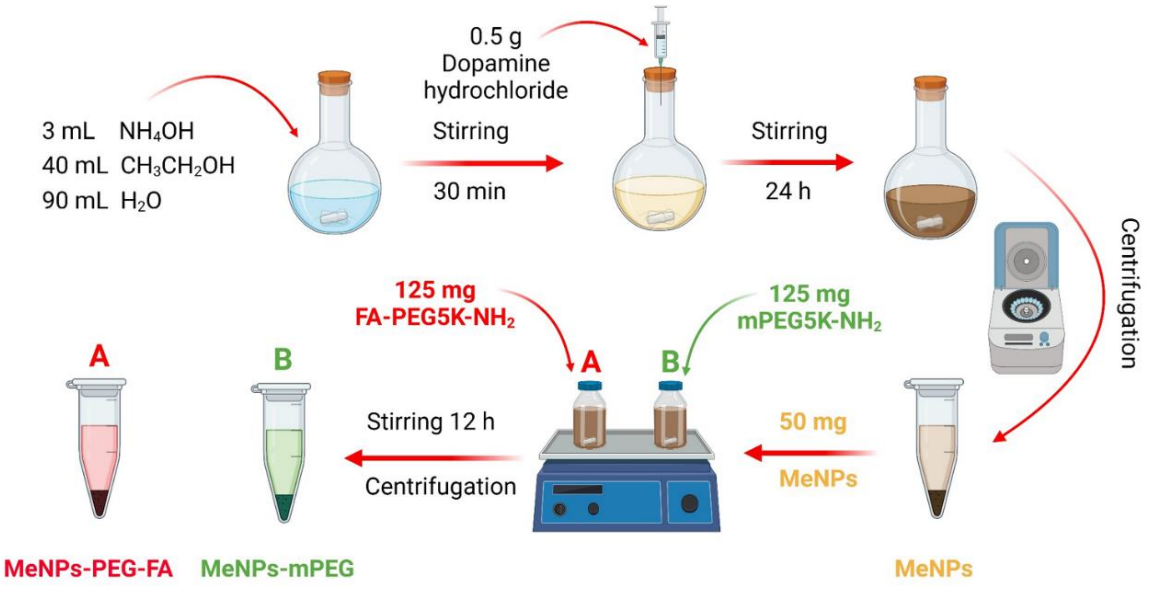

Figure 1. Schematic illustration of the synthesis of MeNPs first and then MeNPs-mPEG and MeNPs-PEG-FA by stirring and centrifugation.

DOI: 10.54254/2755-2721/61/20240921

2.5. Performance testing for scavenging DPPH and superoxide free radicals

For the superoxide free radical scavenging experiment, 1.0 mL of the sample solution with different concentrations (0-300 $\mu g \cdot mL^{-1}$) and 0.3 mL of the 15.0 $mmol \cdot L^{-1}$ pyrocatechol solution were added, in sequence, to 3.7 mL Tris-HCl (pH=8.2) buffer solution. The absorbance A_1 at 420 nm was measured after 20 min in a 25 ℃ water bath. The scavenging rate of superoxide anion radical was calculated by the formula.

Superoxide radical clearance rate (%) = $(A_0 - A_1)/A_0 \times 100$. In the formula, A_0 is the absorbance value of ultra-pure water replacing the sample as the blank group.

For the DPPH free radical scavenging experiment, 2 mL of samples with different concentrations were successively added to 2 mL of DPPH solution (0.2mM). The mixture was then mixed and allowed to react at room temperature for 30 minutes. After the reaction, the absorption value A_1 was determined at 535 nm wavelength. The scavenging rate of DPPH free radical can be obtained by calculation.

DPPH free radical scavenging rate (%) = $(A_0 - A_1)/A_0 \times 100$, where A_0 is the light absorption value of 2 mL 95% ethanol plus 2 mL DPPH solution.

2.6. Cell Counting Kit-8 to test cell cytotoxicity

When RAW264.7 cells reached 95% confluence in the cell culture dish, the cells were pipetted off and collected by centrifuge at 200 g for 5 min. Cells counting was performed to determine RAW264.7 cells number. RAW264.7 cells were resuspended in medium with a concentration of 5×10^4 per mL. Then 100 μL of the RAW264.7 cell suspension was inoculated into each well of a 96-well plate. For cytotoxicity tests, 5000 cells were added to each well in a volume of 100 μL. The experimental group was cultured as required and treated with 0.1, 0.2, 0.5, 1, 2, and 3 μL of MeNPs-mPEG or MeNPs-PEG-FA with both at a concentration of 10 $\mu g\ \mu L^{-1}$. This resulted in final concentrations of 10, 20, 50, 100, 200, and 300 $\mu g\ mL^{-1}$ of MeNPs-mPEG or MeNPs-PEG-FA per well, respectively. After 24 hours of incubation, 10 μL of CCK-8 solution was added to each well, and the plate was further cultured in the cell incubator for 2 hours. The absorbance was measured at a wavelength of 450 nm with a microplate reader.

2.7. Flow cytometry to determine the efficiency of cells uptake

When the cells grew to 95% confluence in the cell culture dish, RAW264.7 cells were pipetted off and collected by centrifugation at 200 g for 5 min. Cell counting was performed to determine the number of RAW264.7 cells. RAW264.7 cells were re-suspended in medium with a concentration of 1×10^6 per mL. Then RAW264.7 was inoculated on the 6-well plate at 1 mL per well. The appropriate amount of lipopolysaccharide (LPS), FITC-conjugated MeNPs-mPEG, LPS with FITC-conjugated MeNPs-mPEG, FITC-conjugated MeNPs-PEG-FA, LPS with FITC-conjugated MeNPs-PEG-FA were added to the wells to achieve a final concentration of 25 $\mu g \cdot mL^{-1}$ of LPS and 10 $\mu g \cdot mL^{-1}$ of MeNPs. The control group was leaved untreated. The 6-well plate was cultured in CO_2 incubator for 24 hours. The RAW264.7 cells were washed with PBS buffer for three times after culture then collected by centrifuge at 200 g for 5 minutes. The cells were then resuspended in FACS buffer (1% FBS PBS) and transferred to FACS tubes. The cell suspension was thoroughly mixed and tested by flow cytometry.

2.8. Quantitative polymerase chain reaction

RNA was extracted with Trizol method by using RNA isolater Total RNA Extraction Reagent (R401-01, Vazyme). cDNA was obtained using HiScript 1st Strand cDNA Synthesis Kits (R111-01, Vazyme), followed by real-time quantitative PCR (qPCR). The cDNA obtained by reverse transcription was diluted 10 times with sterilized water at a concentration of 100 ng/μL and transferred into 1.5 mL EP tube. Take the 96-well plate and design the sampling position according to the number of samples. Upstream and downstream primers can be premixed in advance, 2 μL of upstream and downstream primers mix were directly added to the reaction system at the final primer concentration of 10 μM. and 8 μL SYBGreen mix was added to the above complex and placed on ice. Next, 1 μL cDNA was added to each well of the reaction tube, ensuring it reached the bottom of the tube. The 96-well plate was

DOI: 10.54254/2755-2721/61/20240921

centrifuged instantly at 1000 rpm to ensure that the reaction liquid settled at the bottom of the wells. Quantitative polymerase chain reaction was performed with LC480 (Roche).

2.9. Evaluation of intracellular clearance of RONS with DCFH-DA

After the cell coverage reached 95% in the cell culture dish, RAW264.7 cells were harvested and centrifuged at 200 g for 5 minutes. The cell counts of RAW264.7 was determined. RAW264.7 cells were then re-suspended in medium with a concentration of 1×10^5 per mL. Next, the cell suspension was added into six 3.5 cm diameter petri dishes at 1 ml per well then cultured in CO_2 incubator for 24 hours. To each culture dish, 10 μL of LPS, MeNPs-mPEG, LPS with MeNPs-mPEG, MeNPs-PEG-FA, LPS with MeNPs-PEG-FA was added at a concentration of 10 μg μL^{-1}. The control group was added with same volume of DMEM medium. At this point, six petri dishes were placed in an incubator at 5% CO_2 and 37℃ for 2 hours to stimulate the cells with the materials or LPS. Each petri dish was then stained with 5 μM of RONS probe DCFH-DA and cultured in incubator under the same conditions for 20 minutes. Then, the petri dishes were washed three times with PBS to remove excess DCFH-DA outside the cells. Finally, a scanning laser confocal microscope was applied to observe and record the samples.

3. Results and Discussion

3.1. Synthesis and characterization

Melanin nanoparticles (MeNPs) were synthesized by mixing them with water, ethanol, and ammonia, where their oxidation reaction and self-polymerization could take place at room temperature. To delve into the intricacies of their structure, Transmission Electron Microscopy (TEM) analysis was conducted. As shown in **Figure 1a** and **Figure 1b**, the TEM images of MeNPs exhibited the monodisperse nanospheres with the typical sphaerolitic structure **(Figure 2a** and **Figure 2b)** [20-22]. Furthermore, the introduction of mPEG5k-NH2 and FA-PEG5k-NH2 resulted in the creation of MeNPs-mPEG and MeNPs-PEG-FA, respectively. Employing TEM once more, MeNPs-mPEG **(Figure 2c** and **Figure 2d)** and MeNPs-PEG-FA **(Figure 2e** and **Figure 2f)** were observed to exhibit remarkable dispersion and maintain uniform particle dimension. This observation serves to validate the robustness of the MeNPs' structure against the modifications introduced by mPEG and PEG-FA moieties, affirming the basic structure of the MeNPs is not changed [19].

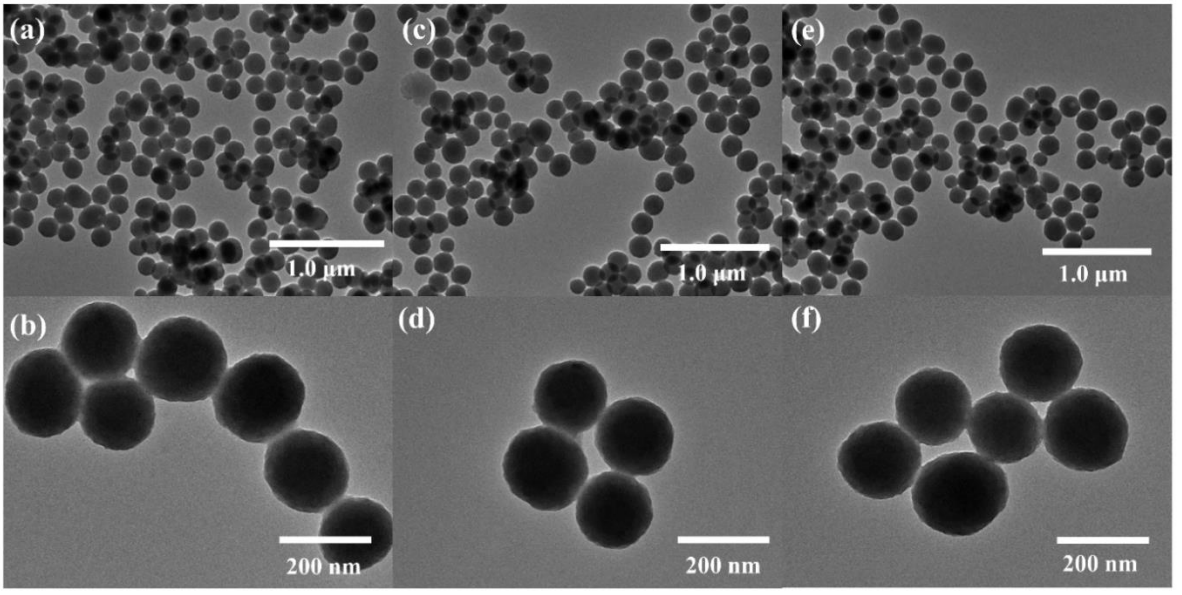

Figure 2. (a) and (b) TEM image of MeNPs, (c) and (d) TEM image of MeNPs-mPEG. (e) and (f) TEM image of MeNPs-PEG-FA.

DOI: 10.54254/2755-2721/61/20240921

To validate the surface modification of MeNPs, the hydrodynamic diameter and zeta potential of MeNPs, MeNPs-mPEG, MeNPs-PEG-FA were measured. As shown in **Figure 3a** and **Figure 3f**, the mean hydrodynamic diameter and zeta potential of MeNPs were 212.6 ± 1.9 nm and -31.6 ± 1.67 mV. When mPEG was loaded, the resultant MeNPs-mPEG demonstrated the increased hydrodynamic diameter (244.97 ± 3.52 nm) and zeta potential (-25.27 ± 0.29 mV) **(Figure 3b)**. Furthermore, after the surface modification of PEG-FA, the mean hydrodynamic diameter further increased to 267.1 ± 6.24 nm, while the zeta potential changed to -17.6 ± 0.79 mV **(Figure 3c)**. All the variation of hydrodynamic diameter and zeta potential during the surface modification of nanoparticles verify the sequentially introducing mPEG and PEG-FA. This transition in zeta potential values can be attributed to the encapsulation of MeNPs by mPEG and PEG-FA, effectively concealing the surface charge and thus resulting in an augmented zeta potential **(Figure 3d)**.

In the measurement of size distribution, as shown in the **Figure 3e**, the Polymer Dispersity Index (PDI) unveils insights into the homogeneity of particle sizes. Upon introducing new groups to the MeNPs, as seen in MeNPs-mPEG and MeNPs-PEG-FA, a phenomenon of increasing PDI becomes apparent. This increase in PDI is attributed to the expansion of particle diameters due to the added groups. Consequently, the PDI values measured were 0.065 for MeNPs, 0.186 for MeNPs-mPEG, and 0.182 for MeNPs-PEG-FA. Notably, even in light of the rising trend in PDI, the small magnitude of 0.182 for MeNPs-PEG-FA reinforces the robust structural integrity of these modified nanoparticles.

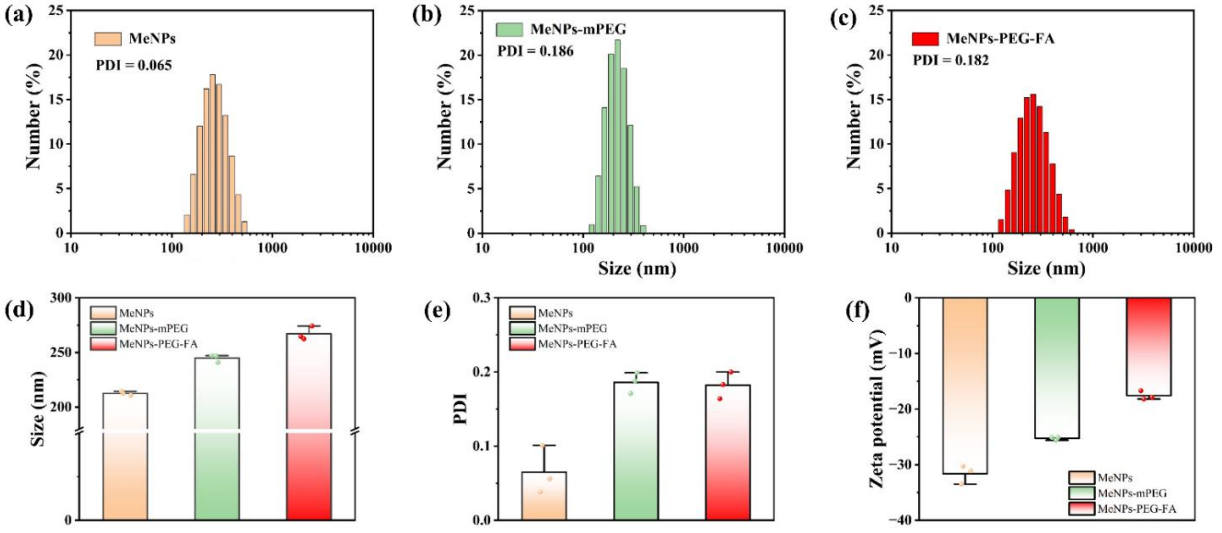

Figure 3. Hydrodynamic diameter image of (a) MeNPs, (b) MeNPs-mPEG and (c) MeNPs-PEG-FA. (d) Hydrodynamic diameter, (e) PDI, (f) Zeta potential of sample MeNPs, MeNPs-mPEG and MeNPs-PEG-FA.

The ultraviolet absorption diagrams of MeNPs, MeNPs-mPEG, and MeNPs-PEG-FA are shown in the **Figure 4a**. The appearance of the absorption in the UV region of the light spectrum was attributed to the oxidation of dopamine into dopachrome and dopaindole, and the following self-polymerization process led to a pronounced absorption extending from visible to NIR wavelengths. So, the three synthesized samples, MeNPs, MeNPs-mPEG, and MeNPs-PEG-FA, all have a wide range of absorption from ultraviolet (UV) to near-infrared (NIR) wavelengths [18].

To validate whether FA was introduced on the surface of MeNPs-mPEG, the MeNPs, MeNPs-mPEG and MeNPs-PEG-FA were characterized with via Fourier transform infrared (FTIR) spectroscopy **(Figure 4b)** to check on the presence of the functional groups from the FA molecule [23]. The characteristic absorbance vibrational peaks for MeNPs-PEG-FA at 845 and 945 cm^{-1} (maybe attributed to the N-H motions in FA), 1480 cm^{-1} (absorption band of the phenyl ring in FA) and ~1650 cm^{-1} (amide bond, H-N-C=O bending vibrations from FA) correspondingly appeared in the MeNPs-PEG-FA

DOI: 10.54254/2755-2721/61/20240921

nanoparticle **(Figure 4b)** [24]. So this infrared spectral image provides additional evidence for the successful synthesis of MeNPs-PEG-FA and MeNPs-mPEG.

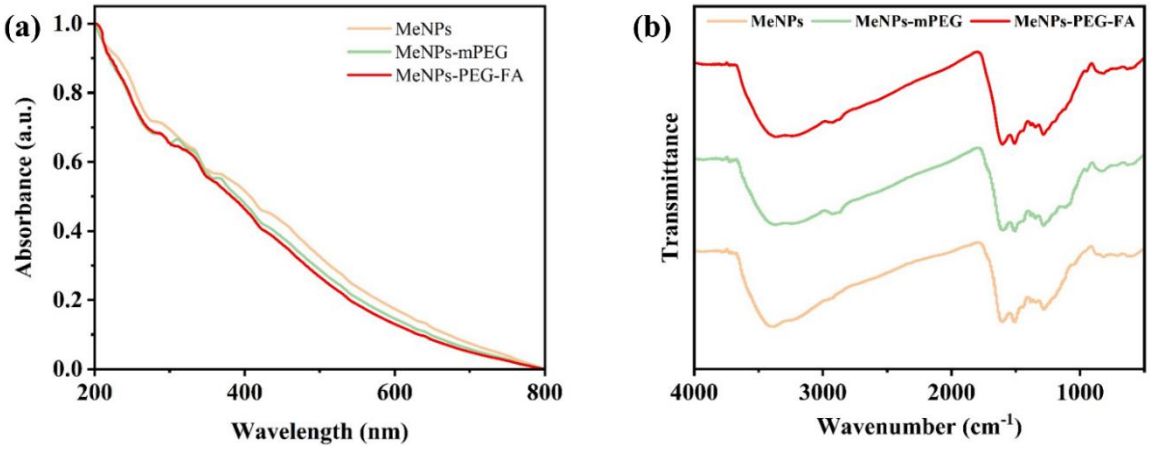

Figure 4. (a) UV-vis absorption spectra of MeNPs, MeNPs-mPEG and MeNPs-PEG-FA. (b) FT-IR spectra of MeNPs, MeNPs-mPEG and MeNPs-PEG-FA.

3.2. Scavenging RONS test

DPPH free radicals and superoxide free radicals are common free radicals in the human body, too many of these free radicals will cause a variety of harm to our body, produce difficult diseases and so on. At the same time, these two free radicals are also the key factors aggravating the disease in RA site. Therefore, through the study of scavenging ability, it was found that MeNPs-PEG-FA had scavenging ability on DPPH free radicals and superoxide free radicals extracellularly [25].

The DPPH radical scavenging experiments of the materials were tested by UV method, as shown in **Figure 5a** is the UV absorption graph of scavenging DPPH radicals of MeNPs-mPEG, and **Figure 5b** is the UV absorption graph of scavenging DPPH radicals of MeNPs-PEG-FA, and the ability of scavenging DPPH radicals of MeNPs-PEG-FA was slightly higher than that of MeNPs- mPEG **(Figure 5c)**, so this set of UV absorption diagrams proved that MeNPs-PEG-FA has some ability to scavenge DPPH radicals. The ability of the materials to scavenge superoxide radicals was tested by the UV method, **Figure 5d** shows the UV absorption graph of MeNPs-mPEG for scavenging superoxide radicals, and **Figure 5e** shows the UV absorption graph of MeNPs-PEG-FA for scavenging superoxide radicals at the same concentration. As shown in **Figure 5f**, the scavenging ability of MeNPs-PEG-FA was slightly higher than that of MeNPs-mPEG. The results of scavenging superoxide radicals were similar to those of scavenging DPPH radicals, but the scavenging ability of MeNPs-PEG-FA no longer increased at concentrations higher than 250 $\mu g \cdot mL^{-1}$.

DOI: 10.54254/2755-2721/61/20240921

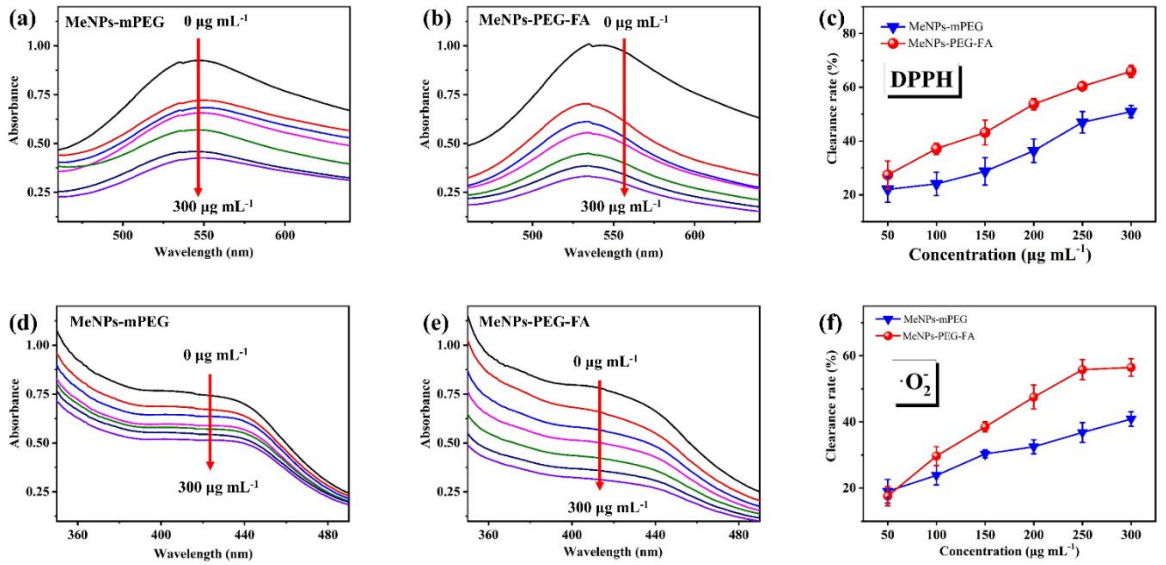

Figure 5. UV-vis absorption diagram of (a) MeNPs-mPEG and (b) MeNPs-PEG-FA scavenging DPPH free radicals. (c) Comparison of DPPH free radical clearance rates of MeNPs-mPEG and MeNPs-PEG-FA. UV-vis absorption diagram of (d) MeNPs-mPEG and (e) MeNPs-PEG-FA scavenging superoxide radical. (f) Comparison of superoxide radical clearance rates of MeNPs-mPEG and MeNPs-PEG-FA.

3.3. In vitro cellular uptake

Targeting is essential for drugs to play a part to eliminate inflammatory response with higher efficacy and fewer adverse reactions. To study the ability of materials to target and enter cells of interest, fluorescence labeled MeNPs-PEG-FA are used to track the distribution within cells [26]. As shown in the histogram **(Figure 6a)**, the FITC-conjugated MeNPs-mPEG treated cells showed a strong fluorescence signal, and the peak of LPS with FITC-conjugated MeNPs-mPEG had a significant shift to the right compared to LPS. Moreover, the cells treated with FITC-conjugated MeNPs-PEG-FA had an even stronger fluorescence signal, and the peak of LPS with FITC-conjugated MeNPs-PEG-FA also exhibits positive shift, which indicated that MeNPs-PEG-FA can be effectively uptake by RAW264.7 cells.

3.4. In vitro cytotoxicity

The determination of cell viability provides insights into cell proliferation and the impact of various substances on cellular health. On this account we applied CCK-8 assay to evaluate the effect of MeNPs-PEG-FA on the viability of two different cell lines (HUVEC cells and RAW264.7 cells) [27]. CCK-8 kits utilize WST-8 as an indicator of cell viability. Briefly, intracellular dehydrogenase catalyzes a REDOX reaction in the presence of an electron carrier, resulting in the production of a water-soluble orange formaldehyde dye that can be quantified in the medium. The intensity of dye formation directly correlates with the number of viable cells.

Experimental findings demonstrated the negligible impact of MeNPS-PEG-FA on cell viability. In HUVEC cells, concentrations of 10, 20, and 50 μg mL^{-1} maintained over 90% cell survival with slight decreases observed at higher concentrations. Notably, even at the highest concentration (300 μg·mL^{-1}), cell viability remained above 85%, indicating minimal drug-induced toxicity **(Figure 6b and Figure 6c)**. Then there is a certain difference between the cell vitality at concentration of 10 μg·mL^{-1} and 300 μg·mL^{-1}, and the original data of 10 μg·mL^{-1} is about 92 and 300 μg·mL^{-1} is about 85. The initial state of cell culture may cause the effects to be magnified. At the same time, this difference was similar to the effect of the drug on cell viability in the other groups, which also indicated that the drug was very low in cytotoxicity. Furthermore, similar results were observed when conducting experiments with

DOI: 10.54254/2755-2721/61/20240921

RAW264.7 cells. Cells treated with MeNPs-PEG-FA at concentration of 10, 20, and 50 μg·mL^{-1} exhibited more than 100% cell viability, which was an indication of that cells even proliferate with materials treating. Remarkably, even at a concentration as high as 300 μg·mL^{-1}, RAW264.7 cell survival rate remained above 90%, suggesting little adverse effects on cellular activity. Similarly, in the MeNPs-mPEG group, the viability of RAW264.7 cells and HUVEC cells could be maintained above 90% at concentrations of 10, 20, and 50 μg·mL^{-1}. Although there was a slight decrease in cell viability with increasing drug concentration, the overall viability remained above 80% **(Figure 6d and Figure 6e)**. Moreover, the result also showed that MeNPs-PEG-FA seems to be less toxic to RAW264.7 than MeNPs-mPEG. These observations collectively demonstrate that both MeNPS-mPEG and MeNPS-PEG-FA are biocompatible—a safe pharmaceutical agents.

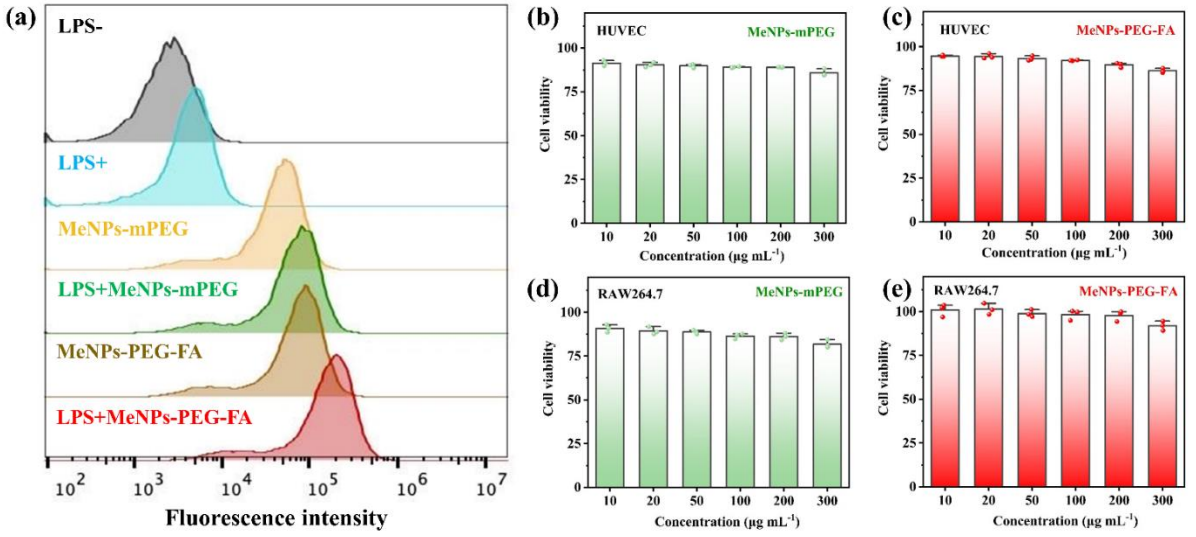

Figure 6. (a) Flow cytometry images of RAW264.7 cells and activated RAW264.7 cells after incubating with FITC-labelled MeNPs-PEG-FA or MeNPs-mPEG for 2 h. *In vitro* viability test of (b) HUVEC cells and (d) RAW264.7 cells in presence of different concentrations of MeNPs-mPEG after 48 h incubation. *In vitro* viability test of (c) HUVEC cells and (e) RAW264.7 cells in presence of different concentrations of MeNPs-PEG-FA after 48 h incubation.

3.5. In vitro RONS scavenging capability

RONS are harmful compounds that can be produced by reactive oxygen and nitrogen radicals. With strong oxidation, it can damage the tissues and cells of the body, and then aggravate the condition of RA and cause other chronic diseases [28, 29]. To determine if MeNPS could decrease the level of RONS within cells, DCFH-DA reagent was applied as an indicator which possesses fluorescence when encountered with RONS in cells. In short, DCFH-DA reagent used has no fluorescence itself, and can freely pass through the cell membrane and enter the cell, and can be hydrolyzed to DCFH by the esterase in the cell. DCFH cannot permeate the cell membrane, making it easy for the probe to be loaded into the cell. Intracellular reactive oxygen species can oxidize non-fluorescent DCFH to produce fluorescent DCF. The intensity of DCF fluorescence could tell the level of intracellular reactive oxygen species. As shown in the fluorescent images **(Figure 7)** of RAW 264.7 cells, LPS with FITC-labelled MeNPs-PEG-FA or LPS with FITC-labelled MeNPs-mPEG have very little fluorescence emission compared to cells activated only by LPS. In particular, the group labelled with FITC-labelled MeNPs-PEG-FA is less than the group labelled with FITC-labelled MeNPs-mPEG. This shows that the RONS content in the MeNPs-PEG-FA treated group is extremely small. It was also well proved that MeNPs-PEG-FA has a good ability to clear RONS free radicals in cells, and has a good potential to treat RA.

DOI: 10.54254/2755-2721/61/20240921

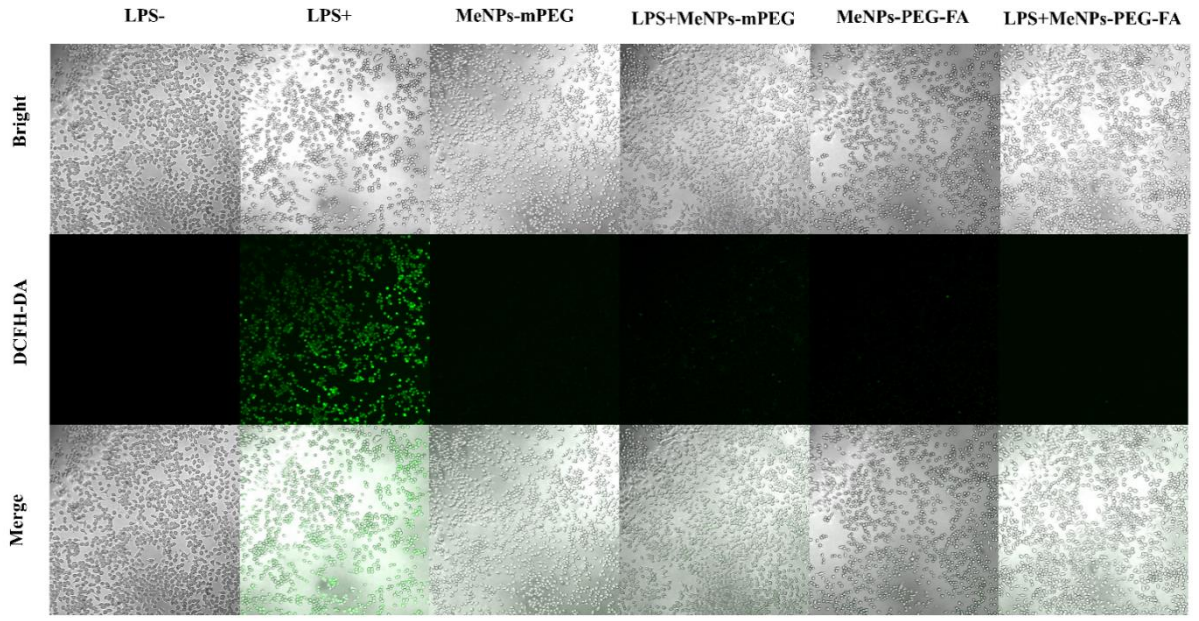

Figure 7. Fluorescent images of RAW 264.7 cells and activated RAW 264.7 cells (by LPS) treating with MeNPs-PEG-FA or MeNPs-mPEG or FITC-labelled MeNPs-PEG-FA or FITC-labelled MeNPs-mPEG for 2 hours.

3.6. Intracellular inflammatory factors

TNF-α is the earliest and most important inflammatory mediator in the inflammatory response process, which increases the permeability of vascular endothelial cells and promotes the synthesis and release of other cytokines. IL-6, an important cytokine which produced mainly by mononuclear macrophages, is continuously and abnormally synthesized in local tissues, which can lead to body fever, inflammatory reaction and pathological changes of some diseases. These inflammatory factors are also one of the causes of RA symptoms, so eliminating inflammatory factors can alleviate the symptoms of RA. The change of intracellular inflammatory factors before and after treatment can strongly prove the therapeutic effect of RA [30, 31].

The quantitative PCR technology uses primers to amplify the target DNA sequence, and uses fluorescent dye method to detect the number of PCR products to quantitatively analyze the number of inflammatory factors expressed in the sample. In the experiment of TNF-α, it can be seen that only in LPS, the relative expression of inflammatory factors reaches 120. However, in the LPS with MeNPs-mPEG group, the relative expression of TNF-α was only about 8, which decreased by about 15 times. The expression of TNF-α was lower in the LPS with MeNPs-PEG-FA group, about 20 times lower than that of LPS only **(Figure 8a)**. Similarly, in the experiments with IL-6, an inflammatory factor, the relative expression in the LPS only group was about 110. In the LPS with MeNPs-mPEG group, the expression of IL-6 was only about 18, a decrease of about 6-fold. In the group of LPS with MeNPs-PEG-FA, the relative expression of IL-6 was even lower, dropping about 8-fold from the LPS-only group **(Figure 8b)**. The data suggest that, all together, down-regulated inflammatory cytokines indicate that MeNPs-PEG-FA drugs have an inhibitory effect on inflammatory pathways and can alleviate inflammatory symptoms.

DOI: 10.54254/2755-2721/61/20240921

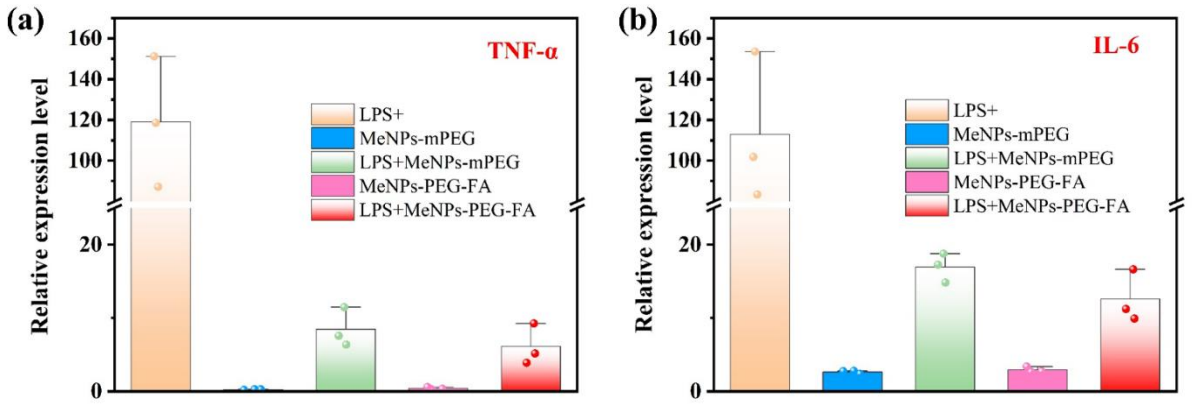

Figure 8. The mRNA levels of (a) TNF-α in activated macrophages treated with LPS, MeNPs-mPEG, LPS with MeNPs-mPEG, MeNPs-PEG-FA, LPS with MeNPs-PEG-FA. And (b) the mRNA levels of IL-6 in activated macrophages treated with LPS, MeNPs-mPEG, LPS with MeNPs-mPEG, MeNPs-PEG-FA, LPS with MeNPs-PEG-FA.

4. Conclusion

In conclusion, MeNPs-PEG-FA is expected to be a new drug for the treatment of RA and will be of great help to the development of targeted therapies for RA. There are a variety of complex factors interacting in the RA microenvironment, and an innovative approach needs to be proposed in order to alleviate the symptoms of RA, such as synovitis, vascular opacities, and bone damage. But at the same time, there are still some limitations, such as the early diagnosis of RA is difficult, early diagnosis is mainly based on clinical symptoms. However, through the blood test is not necessarily positive, the general onset of 6-8 months to find out, the treatment is more difficult and the effect is generally not ideal. As designed in this study, MeNPs-PEG-FA can increase the targeting of this drug to reach the inflammation site precisely. Moreover, our test experiments have also demonstrated that MeNPs-PEG-FA has very low toxicity to cells, good biosafety, good cellular uptake, and strong free radical uptake capacity. Thus, by utilizing these properties of MeNPs-PEG-FA, this drug can reduce oxidative stress and inhibit inflammation, thereby reducing the symptoms associated with RA. As we continue to explore, this innovative treatment is also expected to provide new hope for patients battling RA.

References

[1] SAVTEKIN, G.; ŞEHIRLI, A. Ö. Rheumatoid arthritis in temporo-mandibular joint: a review. *Nigerian Journal of Clinical Practice*, 2018, 21(10): 1243-1246.

[2] SODHI, Amandeep, et al. Rheumatoid arthritis affecting temporomandibular joint. *Contemporary clinical dentistry*, 2015, 6(1): 124-127.

[3] Roth G A, Abate D, Abate K H, et al. Global, regional, and national age-sex-specific mortality for 282 causes of death in 195 countries and territories, 1980–2017: a systematic analysis for the Global Burden of Disease Study 2017. *The Lancet*, 2018, 392(10159): 1736-1788.

[4] RATHORE, Brijesh, et al. Indian herbal medicines: Possible potent therapeutic agents for rheumatoid arthritis. *Journal of clinical biochemistry and nutrition*, 2007, 41.1: 12-17.

[5] MRID, Reda Ben, et al. Anti-rheumatoid drugs advancements: New insights into the molecular treatment of rheumatoid arthritis. *Biomedicine & Pharmacotherapy*, 2022, 151: 113126.

[6] DE MOLON, Rafael Scaf, et al. Linkage of periodontitis and rheumatoid arthritis: current evidence and potential biological interactions. *International journal of molecular sciences*, 2019, 20(18): 4541.

[7] WANG, Xing, et al. The role of reactive oxygen species in the rheumatoid arthritis-associated synovial microenvironment. *Antioxidants*, 2022, 11(6): 11061153.

DOI: 10.54254/2755-2721/61/20240921

[8] ZHAO, Tianqi, et al. Spinel-type persistent luminescence nanoparticles: From mechanisms, compositions to applications. *Coordination Chemistry Reviews*, 2023, 488: 215171.
[9] JEONG, Mini, et al. Hempseed oil induces reactive oxygen species-and C/EBP homologous protein-mediated apoptosis in MH7A human rheumatoid arthritis fibroblast-like synovial cells. *Journal of Ethnopharmacology*, 2014, 154(3): 745-752.
[10] NAKAJIMA, Shotaro; KITAMURA, Masanori. Bidirectional regulation of NF-κB by reactive oxygen species: a role of unfolded protein response. *Free Radical Biology and Medicine*, 2013(65): 162-174.
[11] CHEN, Ming-Wa, et al. NIR-PTT/ROS-scavenging/oxygen-enriched synergetic therapy for rheumatoid arthritis by a pH-responsive hybrid CeO_2-ZIF-8 coated with polydopamine. *ACS Biomaterials Science & Engineering*, 2022, 8(8): 3361-3376.
[12] PARK, Yune-Jung; YOO, Seung-Ah; KIM, Wan-Uk. Role of endoplasmic reticulum stress in rheumatoid arthritis pathogenesis. *Journal of Korean medical science*, 2014, 29(1): 2-11.
[13] DIAS, Ivo Ricardo de Seabra Rodrigues, et al. Potential therapeutic compounds from traditional Chinese medicine targeting endoplasmic reticulum stress to alleviate rheumatoid arthritis. *Pharmacological Research*, 2021, 170: 105696.
[14] WANG, Biao, et al. Dopamine D3 receptor signaling alleviates mouse rheumatoid arthritis by promoting Toll-like receptor 4 degradation in mast cells. *Cell Death & Disease*, 2022, 13(3): 240.
[15] FAN, Quli, et al. Transferring biomarker into molecular probe: melanin nanoparticle as a naturally active platform for multimodality imaging. *Journal of the American Chemical Society*, 2014, 136(43): 15185-15194.
[16] ZHANG, Ruiping, et al. Engineering melanin nanoparticles as an efficient drug-delivery system for imaging-guided chemotherapy. *Advanced Materials*, 2015, 27(34): 5063-5069.
[17] CHEN, Ying, et al. Dimethylamino group modified polydopamine nanoparticles with positive charges to scavenge cell-free DNA for rheumatoid arthritis therapy. *Bioactive Materials*, 2022, 18: 409-420.
[18] LIU, Yanlan, et al. Dopamine-melanin colloidal nanospheres: an efficient near-infrared photothermal therapeutic agent for in vivo cancer therapy. *Advanced materials*, 2013, 25(9): 1353-1359.
[19] LIU, Yanlan, et al. Comprehensive insights into the multi-antioxidative mechanisms of melanin nanoparticles and their application to protect brain from injury in ischemic stroke. *Journal of the American Chemical Society*, 2017, 139(2): 856-862.
[20] LIU, Y. A. N.; SIMON, John D. Isolation and biophysical studies of natural eumelanins: applications of imaging technologies and ultrafast spectroscopy. *Pigment cell research*, 2003, 16(6): 606-618.
[21] AI, Kelong, et al. Large-Scale Synthesis of Bi 2 S 3 Nanodots as a Contrast Agent for In Vivo X-ray Computed Tomography Imaging. *Advanced materials*, 2011, 42(23): 4886-4891.
[22] LIU, Yanlan, et al. A high-performance ytterbium-based nanoparticulate contrast agent for in vivo X-ray computed tomography imaging. *Angewandte Chemie*, 2012, 124(6): 1466-1471.
[23] LI, Fulai, et al. Affordable and simple method for separating and detecting ovarian cancer circulating tumor cells using BSA coated magnetic nanoprobes modified with folic acid. *Sensors and Actuators B: Chemical*, 2018, 262: 611-618.
[24] DALIX, Elisa, et al. Similar effect of co-administration of methotrexate and folic acid for the treatment of arthritis compared to separate administration. *Rheumatology*, 2023, 62(4): 1706-1710.
[25] MATEEN, Somaiya, et al. Increased reactive oxygen species formation and oxidative stress in rheumatoid arthritis. *PloS one*, 2016, 11(4): e0152925.
[26] YANG, Modi, et al. Scavenger receptor-mediated targeted treatment of collagen-induced arthritis by dextran sulfate-methotrexate prodrug. *Theranostics*, 2017, 7(1): 97-105.

DOI: 10.54254/2755-2721/61/20240921

[27] DE MATTEIS, Valeria, et al. Negligible particle-specific toxicity mechanism of silver nanoparticles: the role of Ag^+ ion release in the cytosol. *Nanomedicine: Nanotechnology, Biology and Medicine*, 2015, 11(3): 731-739.

[28] KIM, Jonghoon, et al. Synergistic oxygen generation and reactive oxygen species scavenging by manganese ferrite/ceria co-decorated nanoparticles for rheumatoid arthritis treatment. *ACS nano*, 2019, 13(3): 3206-3217.

[29] ZHANG, Qi, et al. Anti-inflammatory and antioxidative effects of tetrahedral DNA nanostructures via the modulation of macrophage responses. *ACS applied materials & interfaces*, 2018, 10(4): 3421-3430.

[30] ZHU, Yan, et al. Rheumatoid arthritis microenvironment insights into treatment effect of nanomaterials. *Nano Today*, 2022, 42: 101358.

[31] CHOY, Ernest H.; KAVANAUGH, Arthur F.; JONES, Simon A. The problem of choice: current biologic agents and future prospects in RA. *Nature Reviews Rheumatology*, 2013, 9(3): 154-163.